THE JOURNAL OF PHYSICAL CHEMISTRY A

ARTICLE

pubs.acs.org/JPCA

The Dynamics of Allyl Radical Dissociation

Chao Chen,[†] Bastiaan Braams,[†] David Y. Lee,[‡] Joel M. Bowman,[†] Paul L. Houston,*[,‡] and Domenico Stranges[§]

[†]Department of Chemistry Emory University Atlanta, Georgia 30322, United States

[‡]School of Chemistry and Biochemistry Georgia Institute of Technology Atlanta, Georgia 30332, United States

[§]Dipartimento di Chimica Università "La Sapienza" P.le A. Moro 5 Rome I-00185, Italy

Supporting Information

ABSTRACT: Dissociation of the allyl radical, CH_2CHCH_2, and its deuterated isotopolog, CH_2CDCH_2, have been investigated using trajectory calculations on an ab initio ground-state potential energy surface calculated for 97 418 geometries at the coupled cluster single and double and perturbative treatment of triple excitations, with the augmented correlation consistent triple-ζ basis set level (CCSD(T)/AVTZ). At an excitation energy of 115 kcal/mol, corresponding to optical excitation at 248 nm, the primary channel is hydrogen loss with a quantum yield of 0.94 to give either allene or propyne in a ratio of 6.4:1. The total dissociation rate for CH_2CHCH_2 is 6.3×10^{10} s^{-1}, corresponding to a $1/e$ time of 16 ps. Methyl and C_2H_2 are produced with a quantum yield of 0.06 by three different mechanisms: a 1,3 hydrogen shift followed by C−C cleavage to give methyl and acetylene, a double 1,2 shift followed by C−C cleavage to give methyl and acetylene, or a single 1,2 hydrogen shift followed by C−C cleavage to give methyl and vinylidene. In this last channel, the vinylidene eventually isomerizes to give internally excited acetylene, and the kinetic energy distribution is peaked at much lower energy (6.4 kcal/mol) than that for the other two channels (18 kcal/mol). The trajectory results also predict the **v**−**J** correlation, the anisotropy of dissociation, and distributions for the angular momentum of the fragments. The **v**−**J** correlation for the CH_3 + HCCH channel is strongest for high rotational levels of acetylene, where **v** is perpendicular to **J**. Methyl elimination is anisotropic, with $\beta = 0.66$, whereas hydrogen elimination is nearly isotropic. In the hydrogen elimination channel, allene is rotationally excited with a total angular momentum distribution peaked near $J = 17$. In the methyl elimination channel, the peak of the methyl rotational distribution is at $J \approx 12$, whereas the peak of the acetylene rotational distribution is at $J \approx 28$.

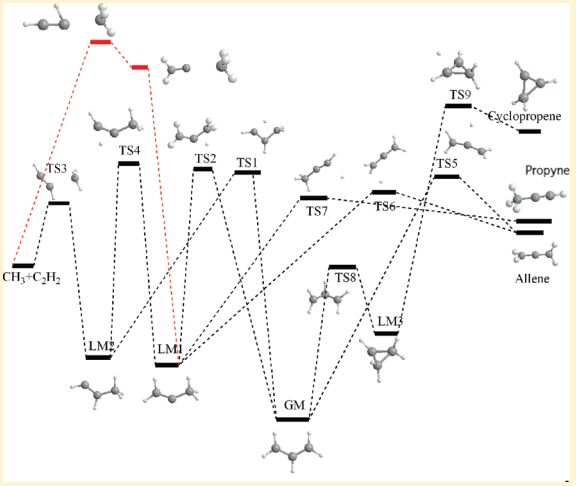

INTRODUCTION

Although the allyl radical (C_3H_5) is important in the combustion mechanisms of hydrocarbons, in planetary atmospheres, and in atmospheric chemistry,[1−6] little is known about the competing dissociation channels for allyl radicals excited with a specific internal energy. Chen and his co-workers advanced the field by developing a pyrolysis source that could dissociate allyl iodide to produce a molecular beam of allyl radicals. Building on early spectroscopic work by Sappey and Weisshaar,[7] the Chen group identified the B[1^2A_1], C[2^2B_1], and D[1^2B_2] states of allyl and some of its deuterated isotopologs using two-photon ionization.[7−10] Subsequent work using similar techniques has characterized several Rydberg states of allyl.[11,12] More recently, some of the original assignments have been revised.[13,14]

The first photodissociation study of the allyl radical was performed by Stranges et al.,[15] who used photofragment translational spectroscopy to examine the products following excitation of allyl at 248 and 351 nm. At 248 nm, the primary dissociation channel was H-atom loss (84%), but CH_3 elimination (16%) was also observed (corrected to 5% subsequently[16]). On the basis of the energy release, the authors proposed that the CH_3 was eliminated directly from a four-center cyclic transition state. Subsequent work[16] with similar techniques, but using CH_2CDCH_2, suggested that there are actually two mechanisms for production of methyl products, each associated with a distinguishable velocity distribution. The theoretical analysis by Davis et al.[17] when compared with the isotopic composition of the measured products[16] suggested an identification of the two methyl elimination

Special Issue: J. Peter Toennies Festschrift

Received: September 29, 2010
Revised: December 6, 2010
Published: January 12, 2011

ACS Publications © 2011 American Chemical Society

channels. In one, a 1,3 hydrogen shift takes place to give the CH_3CDCH intermediate, which then dissociates to yield CH_3 + DCCH, whereas in the second, two 1,2 hydrogen shifts take place, the first to form $CH_2D-C-CH_2$ and the second to form CH_2D-CH−CH, which subsequently dissociates to CH_2D + HCCH. These reactions can be summarized as

$$CH_2CDCH_2 \rightarrow CH_3CDCH \rightarrow CH_3 + CDCH \quad (R1)$$

and

$$CH_2CDCH_2 \rightarrow CH_2DCCH_2 \rightarrow CH_2DCHCH \rightarrow CH_2D + CHCH \quad (R2)$$

Stranges et al.[16] found that the kinetic energy distributions for the DCCH and HCCH were different, with the former peaking at about 16 kcal/mol and the latter peaking at about 6 kcal/mol. This result is surprising because both pathways go through an intermediate of the form (for the nondeuterated species) $CH_3-CH-CH$. A key assumption of the RRKM theory is that energy will be randomized in the potential energy well corresponding to this intermediate before dissociation so that one would expect the two isotopically different products to have nearly the same kinetic energy distributions.

Other photodissociation studies have focused on the hydrogen elimination channel. The Fischer and Chen groups have excited allyl and some deuterated isotopologs near 240 nm and probed the H or D product using picosecond time-resolved laser fluorescence.[18−23] Appearance rates for the H or D products were in the 5×10^7 s^{-1} to $\geq 1 \times 10^8$ s^{-1} range. The measurements suggest that H or D is produced on two time scales, but the resolution was not sufficient for measurement of the faster appearance rate. Since the electronically excited states decay nonradiatively within 9−20 ps,[21,22] it is likely that dissociation occurs on the ground electronic state.

Finally, two groups[24−27] have studied the dissociation of allyl by preparing radicals whose internal energy spans the energy barriers to various dissociation channels. In one case, the excited allyl was prepared by dissociation of allyl iodide at 193 nm, whereas in the other, an isomer, the 2-propenyl radical, was prepared by dissociation of 2-bromopropene at 193 nm. By measuring the translational energy distribution of the iodine or bromine product, the researchers were able to determine the internal energy distribution of the allyl product. Then, by comparing this distribution with that measured for the surviving allyl products, they were able to determine the energy distribution of those allyl radicals that dissociated on the time scale between the preparation and detection. Surprisingly, some allyl radicals with energies up to 15 kcal/mol greater than the barrier to H elimination remained stable.[24,25] This stability was attributed to a centrifugal barrier caused by the large amount of rotational energy imparted to the allyl radical from the dissociation of the allyl iodide. Szpunar et al.[24] also measured the H velocity distribution using Rydberg time-of-flight methods.

Theoretical work on the allyl radical has also advanced. As previously mentioned, Davis et al.[17] calculated a dozen stationary points on the allyl surface at the B3-PW91/6-311G(d,p) level and provided energies and RRKM parameters. Electronic structure calculations were also reported by Deyerl et al.[19] to obtain vibrational parameters to perform RRKM calculations. Most of the geometries were optimized using fourth-order perturbation theory including single, double, and quadruple excitations and employing a 6-31G* basis set. Other stationary points on the surface were calculated by Stranges et al.[16] at the QCISD(T) level and by Calstiglione, Bach, and Chen[23] at the CCSD(T) level.

In this paper, we reexamine the dissociation of the allyl radical using trajectory calculations on a full-dimensional ab initio potential energy surface for the ground electronic state of allyl. Our results provide branching ratios for the various H + C_3H_4 products as well as for the CH_3 + C_2H_2 products. The time scale for the dissociation is found to be ∼16 ps ($1/e$), and the results provide translational, internal energy, angular momentum, and vector correlation distributions for the products. Most importantly, the trajectories suggest that the cause of the lower kinetic energy distribution for the CH_2D + HCCH products observed in the experiments of Stranges et al.[16] is that there is a third channel that contributes to these products, the production of methyl plus vinylidene, CH_2D + CCH_2. A preliminary account of this aspect of the dynamics has recently been reported by us.[28]

COMPUTATIONAL METHODS

Construction of the Potential Energy Surface. The construction of the PES employs procedures developed previously in our group.[29−31] The PES is made explicitly invariant under all permutations of like nuclei, and this property is expressed by the polynomial basis used for the fitting. The polynomials are functions of Morse-type variables y_{ij} given by $y_{ij} = \exp(-r_{ij}/\lambda)$, where r_{ij} is the internuclear distance between nuclei i and j. The associated 3308 coefficients were obtained by standard linear-least-squares fitting to a data set of 97 418 ab initio energies, computed at the coupled cluster single, double, and perturbative treatment of triple excitations (CCSD(T)) with the augmented correlation-consistent polarized triple basis set (aug-cc-pVTZ) as implemented in MOLPRO.[32] The configurations include regions of the C_3H_5 complex, the separated CH_3 + C_2H_2, and the product channels for each of the C_3H_4 isomers and hydrogen. The energies of ∼20 000 fragment channel data are obtained by separating the fragments by ∼8 Bohr and assigning the energy as the sum of their fragment energies. The rms fitting error is, as expected, a function of the total energy. Because the trajectories sample potential values from zero to the total energy of the trajectories, the most relevant potential to consider is actually where the distribution of potential values is a maximum. It turns out for this system (and for every complex molecular system we have examined), this value is roughly on half of the total energy. In the present case, this is roughly 78 kcal/mol, and the rms fitting error at this energy is 2.6 kcal/mol.

As previously mentioned, Stranges and co-workers[16] calculated part of the PES, mainly stationary points describing CH_3+C_2H_2 formation. Castiglione et al.[23] provided a more comprehensive description of stationary points covering the C_3H_4 + H region. Those points were used to check our fitted PES. Figure 1 shows the schematic representation of the C_3H_5 PES. It contains a global minimum (GM), three local minima (LM), nine saddle points (TS), and four fragment channels (CH_3 + C_2H_2, and H elimination to produce the C_3H_4 isomers allene, propyne, and cyclopropene).

The hydrogen loss channels are not barrierless but, rather, have saddle points connecting local minima and fragment configurations. In the CH_3 + C_2H_2 channel, there exist two possible pathways to reach the fragment region. The difference between the two pathways is whether the dissociation samples the potential energy well around LM1. Those that do are counted as contributing to the double 1,2 hydrogen shift channel described in

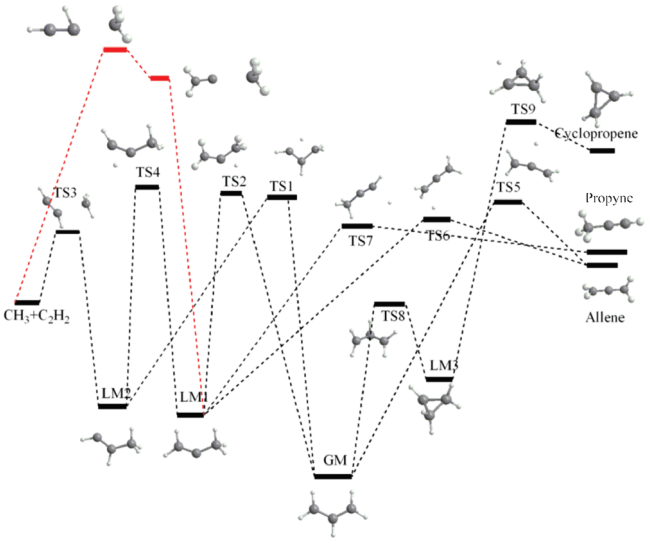

Figure 1. Schematic representation of the allyl potential energy surface.

Stranges et al. (R2),[16] whereas those that bypass this potential energy well are counted as contributing to the 1,3 hydrogen shift channel (R1). These were distinguished by different products when starting with the 2-deuteroallyl radical.[16]

In addition to these two channels, from the molecular dynamics on our PES, we find an unusual mechanism starting from LM1 in which the CH_3CCH_2 dissociates directly to $CH_3 + CCH_2$; the highly excited vinylidene then easily isomerizes over a small barrier to produce internally hot acetylene. The PES describes the isomerization of vinylidene to acetylene via the known saddle point.[33] Overall, the stationary points in our fitted PES agree quite well with ab initio results in terms of geometry, potential energy, and harmonic frequencies. Table 1 give the potential energy comparison between our PES and the ab initio results.[16,23,33] The PES thus seems quite suitable for the quasiclassical trajectory calculations described below. Further details about the PES are given in the supplemental online material for ref 28.

Trajectory Calculations. The quasiclassical trjaectory calculations were performed using methods similar to those used previously.[34] The experimental excitation of the allyl radical produces an excited state that then evolves before internal conversion to the ground PES, and it is not currently known at what geometries this internal conversion takes place. Thus, without further information, we have started most of the trajectories at the geometry of the global minimum of the allyl PES.

Calculations are done in a space-fixed frame using microcanonical sampling of initial momenta subject to the zero total angular momentum constraint. The integration was performed using time steps of 0.1205 fs and were run for typically 200 000 steps or 24.1 ps (in some cases, 100 000 steps or ~12 ps). Approximately 19 000 trajectories were run for CH_2CHCH_2 starting from the global minimum, and ~35 000 trajectories were run for CH_2CD-CH_2 from the global minimum. In addition, for CH_2CHCH_2, mechanistic analysis was facilitated by 2750 trajectories initiated from LM1 and 500 initiated from LM2.

Analysis Methods. Trajectories were analyzed by first assigning a structure to the products. A program automatically classified the final configuration into several categories, such as H + allene, H + propyne, H + other C_3H_4 products, and $CH_3 + C_2H_2$. Since the trajectory keeps track of the identities of the different carbons and hydrogens, it is possible to further categorize the results. Thus, for the $CH_3 + C_2H_2$ category, the products were examined to see whether they were consistent with a 1,3 hydrogen shift mechanism (R1) or a double 1,2 hydrogen shift mechanism (R2). There are multiple variants for each reaction, depending on which hydrogens are transferred.

Once the final structure has been determined, it is a simple matter to determine the relative velocity of the two fragments in the center-of-mass frame. This velocity is used to determine the kinetic energy distribution.

The total orbital angular momentum is determined from the final value of $\mathbf{r} \times \mathbf{p}$ in the allyl center of mass frame. In addition, the angular momentum of each fragment in its own frame may be similarly determined, and all angular momenta can then be converted into units of $\hbar$. Since the starting angular momentum is zero, the vector sum of the orbital momentum and the two fragment angular momenta must also be zero.

It is also possible to determine from the trajectory the projection of the angular momentum of each molecular fragment onto the direction of recoil, since this direction is known from the directions of the linear momenta of the fragments. This projection is sometimes called the $\mathbf{v}-\mathbf{J}$ correlation; it ranges from $\mathbf{v} \| \mathbf{J}$ for helicopter-like motion to $\mathbf{v} \perp \mathbf{J}$ for frisbee-like motion. Mathematically, it is useful to express the result in terms of the bipolar moment $\beta_0^0(22) = P_2(\cos\theta)$, where θ is the angle between $\mathbf{J}$ and the recoil direction, $\mathbf{v}$, and P_2 is the second Legendre polynomial. Note that if one of the fragments, such as H, carries no angular momentum, then $\mathbf{J}$ for the second fragment must be antiparallel to the orbital

Table I. Comparison of the Fitted Potential Energy Surfaces and Ab Initio Benchmark Electronic Energy Calculations for Selected Stationary Points (A) on the C_3H_5 Surface Relative to Allyl Global Minimum (kcal/mol) and (B) on the Part of C_3H_5 Surface Describing Vinylidene and Acetylene Isomerization Relative to Vinylidene Minimum (kcal/mol)

A	QCISD(T)[a]	CCSD(T)[b]	PES
GM	0		0
LM1	19.9		20.4
LM2	23.3		25.0
LM3		32.1	29.5
TS1	67.4		69.6
TS2	67.5	67.2	70.5
TS3	60.8		62.5
TS4	72.0		70.9
TS5		66.9	69.4
TS6		65.1	66.4
TS7		64.3	63.5
TS8		53.2	51.9
TS9		86.1	86.7
HCCH + CH_3	52.6		52.4
allene + H		62.4	62.9
propyne + H		61.1	58.4
cyclopropene + H		84.5	83.5

B	CCSD(TQ)/cc-pvtz[c]	CCSD(T)/ANO[c]	PES
$H_2CC + CH_3$	0	0	0
H_2CC TS + CH_3	2.67	2.87	2.26
HCCH + CH_3	−45.61	−44.10	−45.1

[a] Ref 16. [b] Ref 23. [c] Ref 33.

dx.doi.org/10.1021/jp109344g |J. Phys. Chem. A 2011, 115, 6797–6804

Table II. Comparison of Trajectory Results with Previous Experimental Results

property	C_3H_5 trajectories	CH_2CDCH_2 trajectories	exptl	ref
allene QY	0.80	0.75	0.50−0.75	10
propyne QY	0.12	0.15	0.50−0.25	10
methyl elim (1,3)	0.05	0.08	0.05	16
methyl elim (apparent 1,2)	0.01	0.01		
dissociation Time (ps)	16	23	1000−100,000	18, 19
H vs CH_3 elim	94:6	91:9	95:5	16
D vs H elim		2.9:1	2:1−3:1	10
1,3 vs apparent 1,2 elim	5.6:1	6.1:1	1:1	16

angular momentum, **L**. Since **L** by definition is perpendicular to the recoil velocity, **J** must be, as well. In this case, $\theta = \pi/2$, and $P_2(\cos\theta) = P_2(0) = -0.5$. Thus, $\beta_0^0(22) = -0.5$ for $\mathbf{v}\perp\mathbf{J}$. In the case when $\mathbf{v}\parallel\mathbf{J}$, $\beta_0^0(22) = 1.0$.

Another vector property that can be determined from the trajectories is the anisotropy of fragment recoil in the limit when dissociation is faster than parent rotation. The anisotropy parameter, β, gives the distribution of recoil angles, $I(\theta) \propto 1 + \beta P_2(\cos\theta)$, where θ is the angle between the fragment recoil and the polarization of the dissociation light. The excitation at 248 nm has been assigned by Minsek et al.[8] as being due to a parallel transition with the transition moment along the long or *A* axis of the molecule, the axis about which the moment of inertia is smallest. The trajectories are performed in a space-fixed frame where the *A* axis is initially located parallel to the space-fixed *z* axis. Each trajectory identifies a recoil velocity that makes a specific angle, α, with respect to the *A* axis. The value of the anisotropy parameter, β, to which this angle corresponds is given by $\beta = 2P_2(\cos\alpha)$. Finally, the distribution of trajectories for each product channel gives a distribution of values for β, from which an average may be determined. This value of β would be observed experimentally in the case when the product recoil is fast compared with rotation about an axis perpendicular to that of the transition dipole moment. If the molecule rotates before dissociation, then $I(\theta)$ will become more isotropic, that is, β will be decreased. If the molecule makes three to four rotations about the axis perpendicular to that of the transition dipole moment before dissociation, the distribution will be nearly isotropic.

RESULTS AND DISCUSSION

General Overview. A general overview of the results is taken from a summary of 18 627 trajectories for C_3H_5 and 35 398 trajectories for CH_2CDCH_2 starting from the global minimum. The trajectories were stopped when a dissociation occurred or when they had run for 24 ps. Of these trajectories, ∼18%/28% did not react for C_3H_5/CH_2CDCH_2, respectively, whereas 72%/59% dissociated to give identifiable products. The other 10%/13% visited problematic regions of the potential surface or gave products not easily identified by our computer algorithm. The potential energy surface does contain unphysical regions, usually associated with short internuclear distances. In these very high energy regions, ab initio data may be very sparse or nonexistent, and the nature of the fit may yield unphysical deep negative values. These regions are usually very isolated; however, a small fraction of trajectories do find them. Such trajectories are discarded. Of the trajectories that did dissociate to identifiable products, 80%/75% gave allene, 12%/15% gave propyne, 5%/8% gave methyl + acetylene via an apparent 1,3 hydrogen shift mechanism, 1%/1% gave methyl + acetylene via an apparent double 1,2 hydrogen shift mechanism, and another 1%/2% prduced a C_3-containing product that was not readily identified as allene or propyne. In some cases for this last group, the structure was that of cyclopropene, whereas in others, it was simply a stretched version of allene or propyne. An exponential fit of the number of trajectories undissociated as a function of time gave a $1/e$ decay time for the dissociation of 16 ps for C_3H_5 and 23 ps for CH_2CDCH_2.

The trajectory results are generally in very good agreement with experimental data, although there may be some significant differences. The quantum yields (and branching ratios) for hydrogen and methyl elimination have previously been reported as 95% and 5% (BR = 19.0) for C_3H_5,[16] in excellent agreement with the trajectories, which gave 94% and 6% (BR = 15.7) for C_3H_5 and 91% and 9% (BR = 10.1) for CH_2CDCH_2. Minsek et al.[10] measured the ratio of allene to propyne formation by dissociating the CH_2CDCH_2 allyl isotopolog and measuring the ratio of D to H. Under the assumption that most of the allene is formed by loss of the D, they estimated the allene to propyne ratio to be between 2:1 and 3:1. The trajectory results for D elimination vs H elimination for CH_2CDCH_2 give a ratio of 2.9:1, also in excellent agreement with experiment. The trajectory results indicate that ∼88%/87% of allene formed from C_3H_5/CH_2CDCH_2 dissociation is produced via loss of the central hydrogen. From CH_2CDCH_2, 10.8% of the trajectories that yield propyne also produce deuterium elimination. For the methyl elimination channel, the ratio of reaction R1 to reaction R2 was found experimentally to be ∼1:1/1.6:1,[16] whereas the trajectory results give 5.6:1/6.1:1 for C_3H_5/CH_2CDCH_2. If acetylene produced via the vinylidene channel were more easily ionized than acetylene because of greater internal excitation, the experiment would underestimate this ratio. A summary of these results is provided in Table II.

The one experimental area where it is not easy to reconcile the trajectory results with experiment concerns the dissociation time scale. The trajectories give a $1/e$ time of 16 ps and a dissociation rate of 6.3×10^{10} s^{-1} for C_3H_5 and 23 ps and 4.4×10^{10} s^{-1} for CH_2CDCH_2 (figures summarizing these data are provided in the Supporting Information). In contrast, Deyerl et al.[18,19] measure and calculate a rate on the order of 4.8×10^8 s^{-1} and see changes in the H-vs-D ratio for dissociation of 2-deuteroallyl at times as long as 100 ns. Although there is no obvious way to reconcile these measurements, which differ by several orders of magnitude, it should be noted that the trajectories are run on the ground-state surface, whereas the initial excitation is to an excited surface. From the widths of rotational lines in the excitation spectra,[8−10] Minsek et al. estimate that the internal conversion takes on the order of 20 ps. It is conceivable that some fraction of the population proceeds through intersystem crossing to a long-lived quartet

dx.doi.org/10.1021/jp109344g |*J. Phys. Chem. A* 2011, 115, 6797–6804

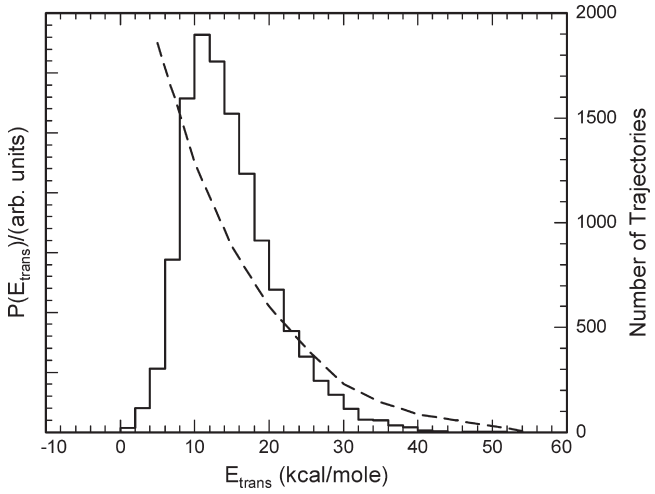

Figure 2. Kinetic energy distribution for hydrogen elimination from C_3H_5. Solid histogram, trajectory results; dashed curve, experimental results from ref 15.

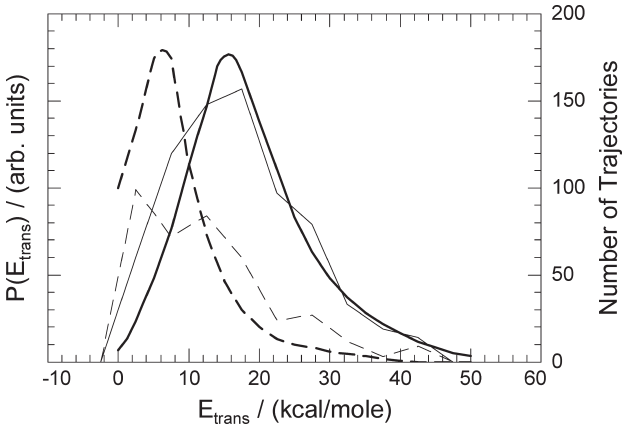

Figure 3. The smooth heavy curves give the experimental kinetic energy distributions for HCCH (dashed, ×3) and DCCH (solid) from ref 16. The light curves give the corresponding distributions for trajectories starting at the allyl global minimum for C_3H_5 (the HCCH distribution has been multiplied by 3).

state and dissociates on the time scale measured by Deyerl et al. However, to give a hydrogen signal that is still small on the nanosecond scale, the fraction of dissociations that follow this hypothetical path must be close to 100%. This explanation would be at odds with the observations that dynamics on the ground state surface correctly predict branching ratios. It should be noted that the dynamics on the excited state are unknown, so that it is unclear where population is transferred from the excited state to the ground state. The trajectory calculations assume that the initial geometry on the ground state is that of the global minimum.

H Elimination Channels. The majority of dissociations produce allene or propyne with H or D elimination. Figure 2 shows the kinetic energy distribution for the hydrogen elimination channels derived from the trajectory results for C_3H_5 along with a distribution obtained from a previous experiment.[16] Although both the current trajectories and the experiments of Stranges et al.[16] use an excitation energy of 115 kcal/mol, the experiments start with allyl radicals that have a rotational temperature of ~50 K due to the use of a pyrolysis source, whereas the trajectories assume that the allyl has zero angular momentum. Thus, this comparison should be made with caution. Despite this difference, it is clear from Figure 2 that the trajectory results are in reasonable agreement with the experimental observation, except at the lowest energies.

Comparison between the trajectory results and two other experiments by Szpunar et al.[24,25] is probably not valid, both because the starting conditions are different and because the total excitation energies are different. The trajectories start with zero angular momentum, whereas the allyl radicals in the experiments of are highly rotationally excited. Szpunar et al.[24,25] have argued that the rotational angular momentum of the allyl radical generated in the dissociation of allyl iodide is responsible for the observation that hydrogen elimination occurs only at energies significantly above the energetic barrier. The trajectory studies are for an excitation energy of 115 kcal/mol, whereas in the experiments of Szpunar et al.,[24,25] the excitation energy is much closer to the threshold for H elimination.

The kinetic energy distributions for the various hydrogen elimination channels from the C_3H_5 trajectories are similar, with the H + propyne and H + other C_3H_4 channels peaking at somewhat lower energy (6−9 kcal/mol) than the distribution for H + allene.

Because the hydrogen product carries no angular momentum, the rotational angular momentum of the allene or propyne must be equal and opposite to the orbital angular momentum, and both rotational vectors must be perpendicular to the recoil velocity; that is, $\beta_0^0(22) = -0.5$. The angular momentum distributions for both the allene and propyne channels peak at about $J = 17$.

Assuming that the allyl radical does not rotate prior to dissociation, the average anisotropy parameters calculated from the trajectories for the allene and propyne channels are −0.14 and −0.08, respectively. Although these values are consistent with the small negative values reported experimentally,[15] −0.05 ± 0.02, the rotational temperature of the allyl in the experiment, ~50 K, is likely to be large enough to influence the anisotropy.

CH_3 Elimination Channels. The methyl elimination channels starting from C_3H_5 and CH_2CDCH_2 were very similar; the P(E) distributions are nearly identical, except for a slight shift to smaller energies for the deuterated methyl, as expected from the slightly larger mass.

Methyl elimination channels were identified by examining the final products to see whether they were consistent with a 1,3 hydrogen shift mechanism (1) or a double 1,2 hydrogen shift mechanism (2). The kinetic energy distributions for these two groups can then be determined separately and compared with the data of Stranges et al.[16] Figure 3 shows that, indeed, the distribution for the dissociation of C_3H_5 via mechanism 1 peaks at a higher kinetic energy (about 16 kcal/mol) than does the distribution for dissociation via mechanism 2. The distributions from the trajectory results are in reasonable agreement with the experimental data. As noted before, this is particularly surprising, since the presumed pathways for reactions R1 and R2 both traverse LM2 before dissociation. The RRKM theory would predict that energy would be randomized in the LM2 potential energy well before dissociation so that the kinetic energy distributions for the products from these two mechanisms should be nearly identical. The reason for the difference will become clear below.

To investigate the methyl elimination channels in more detail, we ran trajectories for C_3H_5 starting from either LM1 or LM2. For all the trajectories that produced methyl, we determined the kinetic energy distribution in each case. The distributions obtained starting in these local minima are similar to those found for the two mechanisms from trajectories starting at the global minimum.

The surprising result, which explains the paradox of why the two kinetic energy distributions are not identical, came from close examination of the trajectories starting from LM1. Those producing methyl were of two kinds: the ones that did the second 1,2 hydrogen shift and those that dissociated directly to vinylidene:

$$CH_3CCH_2 \rightarrow CH_3 + CCH_2 \qquad (R3)$$

In more than one-half of the trajectories starting from LM1 (CH_3CCH_2), the C−C bond broke well before a hydrogen from the CH_2 group migrated to the center carbon. Although the trajectories typically stopped soon after the C−C bond was broken, the CCH_2 clearly had sufficient energy to rearrange to HCCH. On the other hand, the acetylene produced from vinylidene was created with a very large degree of vibrational energy, leaving much less energy available as kinetic energy of recoil. The kinetic energy distribution for the products of a configuration consistent with mechanism (R2) is therefore peaked at lower energy than that for products of a configuration consistent with mechanism (R1). Thus, the trajectory results strongly suggest that the distribution attributed to (R2) actually consists of a mixture of trajectories consistent with (R2) and those consistent with R3. Note that for both reactions R2 and R3 starting with CH_2CDCH_2, the deuterium ends up in the methyl fragment and the acetylene has two hydrogens. Thus, detection of the kinetic energy distributions by mass spectrometry[16] would associate the detection of C_2H_2 to both reactions (R2) and R3 while associating the detection of C_2HD to reaction R1.

The trajectories starting from LM1 may be separated into two groups: those that produce vinylidene and those that undergo the second 1,2 hydrogen shift. The kinetic energy distribution for the products of the latter group is nearly identical to that for trajectories producing products but starting from LM2, as discussed elsewhere.[28] Both distributions have average energies of ∼16 kcal/mol. It thus appears that the RRKM assumption is correct: trajectories passing through the LM2 potential energy well do produce nearly identical kinetic energy distributions, regardless of how they get to this potential energy well.

The kinetic energy distribution for those C_3H_5 trajectories starting in LM1 and producing vinylidene is shown in Figure 4. The distribution peaks near zero and has an average kinetic energy of only 6.4 kcal/mol.

Trajectories starting from the GM and going to LM1 also produced methyl elimination either via the vinylidene channel or the second 1,2 hydrogen shift. Frames from a sample trajectory are shown in ref 28.

It is interesting to investigate why the vinylidene channel is so important, even though its barrier is 26.7 kcal/mol higher than the transition state TS4. An obvious reason is that TS4 requires a very tight configuration in which the hydrogen to be transferred is shared between two carbon atoms. In contrast, the methyl + vinylidene exit channel appears to be much looser. On the other hand, the transition state TS8 to production of H + propyne is also a loose one, so it is surprising that the vinylidene channel can compete.

We attempted to find a transition state barrier between LM1 and $CH_3 + CCH_2$, but it appears that there is simply a monotonic increase in energy between the former and latter. Direct but limited ab initio calculations of the dissociation from LM1 to $CH_3 + CCH_2$ indicate that this dissociation has no barrier beyond that imposed by the endoergicity. Thus, a variational treatment of this channel will be needed for future modeling of the dissociation. Preliminary modeling of this channel by variational transition state theory and use of the information from the PES to determine remaining RRKM rate constants was used to integrate the rate equations and predict branching ratios. The branching ratio to vinylidine + CH_3 is found to be much smaller than that found from the trajectory studies. For example, starting from LM1, the variational RRKM treatment predicts 0.41% vinylidene, whereas the trajectories predict 11%. It is thus clear that the dissociation is nonstatistical at the energy of the dissociation. Additional investigations concerning this somewhat surprising point are underway.[35]

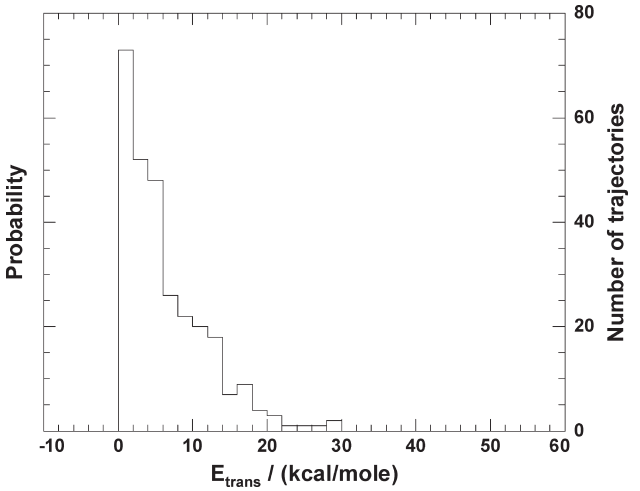

Figure 4. Kinetic energy distribution for those trajectories for C_3H_5 that start in LM1 and produce methyl and vinylidene. The average kinetic energy of this distribution is 6.4 kcal/mol.

A methyl channel that was not prevalent was elimination of methyl radicals containing the carbon atom that was originally located in the center of the allyl molecule. Of 18 627 trajectories for CH_2CHCH_2 starting form the GM, only 5 produced methyl radicals containing the central carbon atom. As might be expected, the mechanism for these 5 trajectories was formation of the cyclical C_3H_5 intermediate LM3 via TS8, followed by H migration within LM3, breaking of the ring back through TS8 to GM, and methyl elimination via one of (R1)−(R3). This rearrangement and dissociation within LM3 does not compete well with the elimination of a hydrogen atom from LM3 to form H + cyclopropene, a process that happened in ∼180 trajectories.

Interestingly, the H that was eliminated to form cyclopropene was *never* the H attached to the central carbon, indicating that H migration within LM3 is slow compared with H loss for our surface. Surprisingly, the barrier to migration has been calculated[35] to be at 75.6 kcal/mol when corrected for zero point energy, somewhat lower than the 86.7 kcal/mol for H loss on our surface to form cyclopropene from the cyclopropyl radical. We did not explicitly examine our surface to determine this migration barrier, so this is an area that will need some further exploration. Experimentally,[16] since there appears not to be scrambling of the deuterium atom in the CH_3CDCH_3 system, it appears that migration in cyclical C_3H_5 is not important.

The angular momentum distributions for methyl and acetylene formed from trajectories traversing the LM2 potential energy well are shown in Figure 5. Also shown are calculated values of $\beta_0^0(22)$ for each of the two products. The acetylene is more rotationally excited than the methyl. For rotational levels in which the rotation of methyl does not contribute, the rotation of the acetylene is balanced by the orbital angular momentum, so that $\beta_0^0(22) \approx 0.5$, indicating that **v** and **J** are nearly perpendicular.

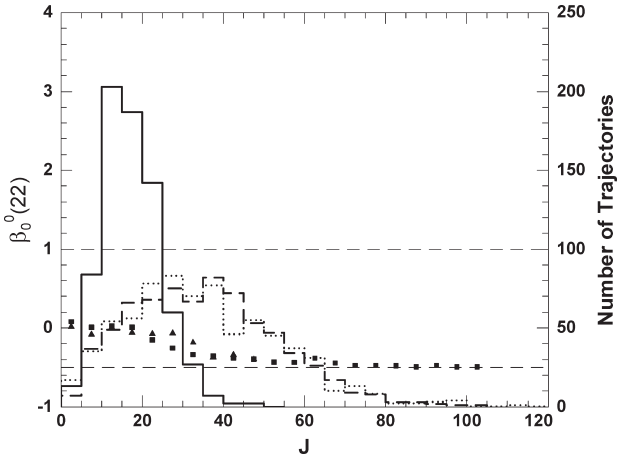

Figure 5. Angular momentum distribution and **v**−**J** correlation for methyl and acetylene produced by trajectories for C_3H_5 passing through the well whose minimum is LM2: the solid line is the methyl distribution; the dotted line is the orbital angular momentum distribution, and the dashed line is the acetylene distribution. $\beta_0^0(22)$ values as a function of J are given for methyl (triangles) and acetylene (squares).

The anisotropy parameter for dissociations producing methyl and acetylene from trajectories traversing the LM2 potential energy well is calculated to be $\beta = 0.66$. For dissociations producing methyl and acetylene from trajectories traversing the LM1 potential energy well (those that produce vinylidene as well as those that produce products via reaction R2), the value of the anisotropy parameter is also calculated to be $\beta = 0.66$.

CONCLUSIONS

The dissociation of allyl radicals has been investigated by constructing a potential energy surface and performing quasiclassical trajectory calculations. Results from the calculations are in reasonable agreement with most available experimental data, although some differences remain. The most important finding is that there are actually three pathways to the methyl plus acetylene products: the two reactions R1 and R2 proposed by earlier research and a third, reaction R3, in which dissociation from LM1 directly to vinylidene takes place. It is this third channel that is responsible for the observed difference in the kinetic energy distribution between different isotopologs of methyl and acetylene.[16] Although this channel has a higher threshold than others, it still plays an important role in the dissociation trajectories, one that seems to be nonstatistical. The trajectory results provide predictions for many properties that have not yet been measured experimentally: specifically, angular momentum distributions, the anisotropy of dissociation, and the **v**−**J** correlation.

ASSOCIATED CONTENT

Supporting Information. Plots of the number of trajectories undissociated as a function of time for both CH_2CHCH_2 and CH_2CDCH_2. This information is available free of charge via the Internet at http://pubs.acs.org/.

AUTHOR INFORMATION

Corresponding Author

*E-mail: paul.houston@cos.gatech.edu.

ACKNOWLEDGMENT

Acknowledgment is made to the Donors of The American Chemical Society Petroleum Research Fund for support in part of this work (No. 46303-AC6). P.L.H. also acknowledges support in part for this work from the National Science Foundation under award CHE-0852482, J.M.B. thanks the Department of Energy under award DE-FG02-97ER14782, and D.S. acknowledges support in part for this work from the Italian Ministero dell'Istruzione, dell'Università e della Ricerca (MIUR, PRIN 2007).

REFERENCES

(1) Huchnall, D. J. *Chemistry of Hydrocarbon Combustion*; Chapman and Hall: London, 1985.
(2) Lara, L. M.; Rodrigo, R.; Coustenis, A.; Lopez-Moreno, J. J.; Chassefiere, E. From European Space Agency, Special Publication, SP 1992, ESA SP-338 (*Proc. Symp. Titan*, 1991), 137-146.
(3) Tulloch, J. M.; Macpherson, M. T.; Morgan, C. A.; Pilling, M. J. *J. Phys. Chem.* **1982,** *86*, 3812–3819.
(4) Fernandes, R. X.; Giri, B. R.; Hippler, H.; Kachiani, C.; Striebel, F. *J. Phys. Chem. A* **2005,** *109*, 1063–1070.
(5) Bentz, T.; Giri, B. R.; Hippler, H.; Olzmann, M.; Striebel, F.; Szöri, M. *J. Phys. Chem. A* **2007,** *111*, 3812–3818.
(6) Jenkin, M. E.; Murrells, T. P.; Shalliker, S. J.; Hayman, G. D. *J. Chem. Soc., Faraday Trans.* **1993,** *89*, 433–436.
(7) Sappey, A. D.; Weisshaar, J. C. *J. Phys. Chem.* **1987,** *91*, 3731–3736.
(8) Minsek, D. W.; Blush, J. A.; Chen, P. *J. Phys. Chem.* **1992,** *96*, 2025–2027.
(9) Blush, J. A.; Minsek, D. W.; Chen, P. *J. Phys. Chem.* **1992,** *96*, 10150–10154.
(10) Minsek, D. W.; Chen, P. *J. Phys. Chem.* **1993,** *97*, 13375–13379.
(11) Wu, J.-C.; Li, R.; Chang, J.-L. *J. Chem. Phys.* **2000,** *113*, 7286–7291.
(12) Liang, C.-W.; Chen, C.-C.; Wei, C.-Y.; Chen, Y.-T. *J. Chem. Phys.* **2002,** *116*, 4162.
(13) Gasser, M.; Schulenburg, A. M.; Dietiker, P. M.; Bach, A.; Merkt, F.; Chen, P. J. *Chem. Phys.* **2009,** *131*, 014304/1–8.
(14) Gasser, M.; Frey, J. A.; Hostettler, J. M.; Bach, A.; Chen, P. *J. Phys. Chem. A* **2010,** *114*, 4704–4711.
(15) Stranges, D.; Stemmler, M.; Yang, X.; Chesko, J. D.; Suits, A. G.; Lee, Y. T. *J. Chem. Phys.* **1998,** *109*, 5372–5382.
(16) Stranges, D.; O'Keeffe, P.; Scotti, G.; Di Santo, R.; Houston, P. L. *J. Chem. Phys.* **2008,** *128*, 151101/1–4.
(17) Davis, S. G.; Law, C. K.; Wang, H. *J. Phys. Chem. A* **1999,** *103*, 5889–5899.
(18) Deyerl, H.-J.; Gilbert, T.; Fischer, I.; Chen, P. J. *Chem. Phys.* **1997,** *107*, 3329–3332.
(19) Deyerl, H.-J.; Fischer, I.; Chen, P. J. *Chem. Phys.* **1999,** *110*, 1450–1462.
(20) Fischer, I.; Chen, P. *J. Phys. Chem. A* **2002,** *106*, 4291–4300.
(21) Schultz, T.; Fischer, I. *J. Chem. Phys.* **1997,** *107*, 8197–8200.
(22) Schultz, T.; Fischer, I. *J. Chem. Phys.* **1998,** *109*, 5812–5822.
(23) Castiglioni, L.; Bach, A.; Chen, P. *Phys. Chem. Chem. Phys.* **2006,** *8*, 2591–2598.
(24) Szpunar, D. E.; Morton, M. L.; Butler, L. J.; Regan, P. M. *J. Phys. Chem. B* **2002,** *106*, 8086–8095.
(25) Szpunar, D. E.; Liu, Y.; McCullagh, M. J.; Butler, L. J.; Shu, J. *J. Chem. Phys.* **2003,** *119*, 5078–5084.
(26) Fan, H.; Pratt, S. T. *J. Chem. Phys.* **2006,** *125*, 144302/1–8.
(27) Fan, H.; Pratt, S. T. *J. Chem. Phys.* **2007,** *127*, 144301/1–8.
(28) Chen, C.; Braams, B.; Lee, D. Y.; Bowman, J. M.; Houston, P. L.; Stranges, D. *J. Phys. Chem. Lett.* **2010,** *1*, 1875–1880.
(29) Brown, A.; Braams, B. J.; Christoffel, K.; Jin, Z.; Bowman, J. M. *J. Chem. Phys.* **2003,** *119*, 8790–8793.
(30) Huang, X.; Braams, B. J.; Bowman, J. M. *J. Chem. Phys.* **2005,** *122*, 044308/1–12.

(31) Xie, Z.; Braams, B. J.; Bowman, J. M. *J. Chem. Phys.* **2005,** *122,* 224307/1–9.
(32) Werner, H. J.; Knowles, P. J.; Lindh, R.; Manby, F. R.; Schutz, M.; Celani, P.; Korona, T.; Rauhut, G.; Amos, R. D.; Bernhardsson, A.; Berning, A.; et al. *MOLPRO,* 1st ed.; 2006.
(33) Chang, N. Y.; Shen, M. Y.; Yu, C. H. *J. Chem. Phys.* **1997,** *106,* 3237–3242.
(34) Shepler, B. C.; Braams, B. J.; Bowman, J. M. *J. Phys. Chem. A* **2008,** *112,* 9344–9351.
(35) Stranges, D.; O'Keeffe, P.; Scotti, G.; Ripani E.; Houston, P. L. Manuscript in preparation.